J. Fluid Mech. (2012), *vol.* 692, *pp.* 112–136.
doi:10.1017/jfm.2011.498

On the cost efficiency of mixing optimization

Oleg Gubanov and Luca Cortelezzi†

Department of Mechanical Engineering, McGill University, Montreal, Quebec, H3A 2K6, Canada

(Received 17 March 2011; revised 22 September 2011; accepted 7 November 2011;
first published online 16 December 2011)

In this study we discuss the cost efficiency of the optimization of a new prototypical mixing flow, the Fourier sine flow, an extension of the sine flow. The Fourier sine flow stirs a mixture on a two-dimensional torus by blinking, at prescribed switching times, two orthogonal velocity fields with profiles represented by a Fourier sine series. We derive a family of mixers of increasing complexity by truncating the series to one, two, three and four modes. We consider the optimization of the velocity profiles and the optimization of the stirring protocol. We implement the former by computing, at each iteration, the amplitudes and phase shifts of the Fourier modes synthesizing the velocity profiles that minimize the mix-norm, our cost function, i.e. maximize the quality of mixing. We implement the latter by selecting, at each iteration, the best performing of the two orthogonal stirring velocity fields, i.e. the velocity field that minimizes the mix-norm. To obtain a physically meaningful optimization problem, we constrain the kinetic energy of the flow to be the same among all mixers and use the viscous dissipation as an estimate of the power input needed to operate the mixers. We characterize the performance of the mixers using three cost functions: the homogenization time, the computational cost of optimization and the total energy consumption. We test the mixers on a range of admissible power inputs using two representative switching times. We report some surprising results. Mixers equipped with the velocity profile optimization and a periodic stirring protocol cannot be optimal, i.e. their performance depends on the switching time chosen, independently of the number of Fourier modes used in the optimization. Apparently, optimal mixers can be obtained only by coupling velocity profile and stirring protocol optimizations. The computational cost of the optimization depends only on the number of Fourier modes used and grows by about an order of magnitude for each Fourier mode added to the optimization. At low power inputs, the coupled optimizations allow us to obtain an attractive reduction of the homogenization time in combination with a reduction of the total energy required to produce it. However, increasing the power input does not guarantee a reduction of the homogenization time. Counter-intuitively, there are ranges of power inputs for which both the homogenization time and the total energy increase when increasing the power input. Finally, for large enough power inputs, optimizations with two, three and four Fourier modes perform similarly, making the former optimization the most cost-efficient.

Key words: chaotic advection, mixing, mixing enhancement

† Email address for correspondence: crtlz@cim.mcgill.ca

1. Introduction

Modern industrial applications demand mixing devices able to achieve a required level of homogenization for a range of operating and initial conditions while minimizing the homogenization time and operating costs. This is especially challenging when mixers must operate in laminar regimes because the design of such mixing devices apparently requires optimization or control of mixing. In recent years, mixing optimization and control have been developed systematically on conceptualized mixers. D'Alessandro, Dahleh & Mezić (1999) considered a mixing device that stirs the mixture on a two-dimensional torus by blinking two steady, orthogonal velocity fields. The device is assumed to be equipped with a sensor that measures the quality of mixing and an actuating system that generates stirring velocity fields with prescribed profiles. The objective of the optimization problem proposed by D'Alessandro *et al.* (1999) is to find an optimal stirring protocol that maximizes the quality of mixing – we will refer to it as *stirring protocol optimization*. D'Alessandro *et al.* (1999) solved the problem for an egg-beater flow that stirs by blinking two orthogonal shear flows, and derived an optimal stirring protocol that maximizes the entropy of the system.

Control of fluid mixing, as formulated by D'Alessandro *et al.* (1999), or the equivalent optimization problem, has been applied in a few studies. Vikhansky (2002*a*,*b*) optimized mixing in a lid-driven cavity flow using optimal control theory. As a cost function, the author used the area of the inter-material boundary (Vikhansky 2002*a*) or the amount of stretching rate along the unstable manifold of the flow (Vikhansky 2002*b*). He reported that these measures of the quality of mixing have some limitations. In particular, the inter-material boundary grows exponentially in a chaotic flow, and so does the computational cost needed to accurately track the interfacial growth (Vikhansky 2002*a*; Mathew, Petzold & Serban 2002). Furthermore, the author noted that high stretching rate along the unstable manifold in general does not imply uniformity of mixing (Vikhansky 2002*b*).

Subsequent studies on optimization and control of mixing have assumed the existence of a sensor able to measure the level of homogenization of the mixture, the mix-norm (Mathew, Mezić & Petzold 2005). The mix-norm is an average, over all scales and locations, of the mean value of the concentration field within a subregion of the mixing domain. Mathew *et al.* (2005) showed that the mix-norm can capture known mixing properties of the processes that mix by chaotic advection and by diffusion. The mix-norm is applicable to mixtures stirred by periodic and aperiodic protocols and is capable of quantifying mixing efficiency in the context of a given initial concentration field. Mathew *et al.* (2007*b*) considered a micromixer that promotes mixing in its main channel by oscillating three secondary transverse flows. The authors determined the amplitudes and frequencies of the oscillating flows that maximize mixing at the outlet of the main channel. Mathew *et al.* (2007*a*) considered the flow induced on a two-dimensional torus by a finite set of prescribed force fields modulated in time. They solved the optimal control problem by finding a protocol that minimizes a weighted sum of the mix-norm and the stirring action per unit mass. Cortelezzi, Adrover & Giona (2008) considered the sine flow (Liu, Muzzio & Peskin 1994), a flow that is stirred within a two-dimensional torus by blinking two orthogonal velocity fields having a sinusoidal profile. The authors introduced a computationally efficient short-time-horizon procedure for the optimization of stirring protocols, and showed that these protocols are nearly as mixing-efficient as the optimal protocol. Gubanov & Cortelezzi (2009) showed that the short-time-horizon optimal protocols are

less sensitive to the geometry of the initial concentration field than the periodic and recursive symmetry-breaking protocols (Liu *et al.* 1994).

The above studies solved the control/optimization problem proposed by D'Alessandro *et al.* (1999) and determined the optimal protocols that maximize mixing by prescribing a time sequence of stirring velocity fields having the same given profile. A complementary control/optimization problem can be formulated as follows. Assuming that the device operates with a periodic protocol, the objective of the optimization problem is to find, at each iteration, the profile of the stirring velocity field that maximizes the quality of mixing. We will refer to this problem as *velocity profile optimization*. The advantage of the stirring protocol optimization is that it only alters the time sequence with which the velocity fields are blinked. On the other hand, the implementation of the velocity profile optimization is obviously more complex because it requires the modification of the actuating system, which should be able to generate different velocity profiles at each iteration.

The two optimization problems described above can be coupled together to form a more complex, but potentially more effective, optimization problem whose objective is to find a stirring protocol and, at each iteration, the profiles of the stirring velocity fields that maximize the quality of mixing. Gubanov & Cortelezzi (2010) considered a simple optimization of the stirring velocity profile of the sine flow. They let the stirring velocity fields slide in the direction transverse to the flow and optimized the lateral translation at each iteration. Although this optimization involves only the lateral translation of the stirring velocity fields without altering their shape, it is highly effective and is essential for achieving a consistent mixing performance for different initial configurations of the concentration field. Gubanov & Cortelezzi (2010) also considered the coupling of this simple velocity profile optimization with the simplest stirring protocol optimization. The authors showed that the coupled optimizations strategy allows for the design of an optimal mixer, i.e. a mixer able to deliver a uniformly optimal mixing performance over a wide range of operating and initial conditions. These results are used as a benchmark in this article.

Most recently, Lin, Thiffeault & Doering (2011) proposed a local-in-time optimization of the velocity field that stirs within an n-dimensional torus. As a quantitative measure of mixing, the authors adopted the H^{-1} norm of the scalar fluctuation field, equivalent to the square root of the variance of a low-pass-filtered image of the concentration field. This norm has the property that halving of all length scales in the tracer distribution leads to a halving of the value of the norm. Using the H^{-1} norm as a cost function, Lin *et al.* (2011) proposed two types of optimizations derived by constraining either the kinetic energy or the viscous dissipation energy of the flow. The authors also derived the lower bounds on the rate at which scalar fields might be mixed. Lin *et al.* (2011) compared their results to the results obtained by Mathew *et al.* (2007*a*) and concluded that expanding the set of available stirring velocity fields increases the mixing performance.

In this study, we consider the velocity profile optimization and its coupling to the stirring protocol optimization in a comprehensive form. To this end, we extend the sine flow (Liu *et al.* 1994), which has been a popular playground for the study of laminar mixing (Pierrehumbert 1994; Antonsen *et al.* 1996; Alvarez *et al.* 1998; Muzzio *et al.* 2000; Szalai *et al.* 2003; Thiffeault, Doering & Gibbon 2004; Phelps & Tucker 2006), by representing with a Fourier series the shape of the profiles of the stirring velocity fields. We call our extension the *Fourier sine flow*, reflecting the nature of the new velocity profiles. We formulate a general velocity profile optimization problem whose objective is to find the amplitude and phase of each harmonic component of the

Fourier sine flow, so that the synthesized velocity profile produces a mixture with the minimal mix-norm value by the end of the time interval over which the stirring field is applied to the flow, the switching time. We couple this optimization with the simplest form of stirring protocol optimization. We implement the latter by selecting, at each iteration, the best performing of the two orthogonal stirring velocity fields, i.e. the velocity field that minimizes the mix-norm. We choose this simple optimization because it has been shown that stirring protocols optimized over a single switching time horizon perform competitively with respect to the stirring protocols optimized over longer horizons (Cortelezzi *et al.* 2008). Note that in the formulation and solution of the optimization problems we use the mix-norm over the H^{-1} norm to allow for an easy comparison with our previous results.

We restrict our study to mixtures having small molecular diffusivity and evolving in laminar regimes. That is, we target flows that have simultaneously high Péclet numbers, i.e. greater than or equal to 10^4, and low Reynolds numbers, i.e. less than or equal to 10. In this physical context, we consider the conceptual design of optimal mixers (Gubanov & Cortelezzi 2010) able to generate the desired level of homogenization in a few characteristic advection times. Under these conditions, mixing is achieved mainly by advection, and diffusion can be neglected. The results presented in this study can be extended to systems with small diffusivity because it has been shown that short-horizon optimal protocols designed for purely advective flows can be robustly transported to advective–diffusive flows of small diffusivities (Cortelezzi *et al.* 2008).

A meaningful solution to the velocity profile optimization problem can be obtained only if the amplitude of the Fourier modes that shape the velocity profile is properly constrained. In the absence of constraints, the optimization routine unboundedly increases the shear rate induced by the stirring velocity field by unboundedly increasing the amplitudes of the Fourier modes. Although unbounded shear rates result in unlimited increase in mixing efficiencies, such increase requires an unlimited power input, which is not available in practical applications.

In physically realizable mixing devices, if one neglects the power lost due to mechanical friction, the power input available is spent to create a shear flow that mixes fluids by inducing stretching and folding. The input energy is partly dissipated by viscous forces and partly transformed into the kinetic energy of the fluid (Malvern 1969). In laminar regimes the former dominates and, consequently, the latter can be neglected (Bigio & Conner 1995). Therefore, we limit the power consumption in our idealized mixing devices by selecting the maximum amount of energy that can be dissipated by viscosity. The implementation of this constraint requires a careful adimensionalization of the problem. The result is an optimization routine that produces realistic results.

We test the mixers on a range of admissible power inputs using two representative switching times and characterize the performance of the mixers using three cost functions: the homogenization time, the computational cost of optimization and the total energy consumption. The first important question we address in this article is the following. Is it possible to design an optimal mixer using the velocity profile optimization alone? One could expect the answer to be ‘yes’, considering that the Fourier sine flow permits efficient reconfiguration of the profile of the stirring velocity fields at each switching time. We will show that this is not the case.

We will also show that optimal mixers can be obtained only by coupling the optimizations of the velocity profiles and stirring protocol. The cost of operating an optimal mixer is hence the sum of the power consumption and the computational

cost of the coupled optimizations. The computational cost, and consequently the total operating cost, increases with the number of Fourier modes included in the velocity profile optimization and the length of the horizon used in the stirring protocol optimization. On the other hand, although expensive, the optimal mixers are expected to reduce the time needed to achieve a desired level of homogenization, i.e. the time needed to decrease the mix-norm from the value associated with the initial concentration field to a given value. These considerations lead to the central question of the present study. When is the reduction in the homogenization time worth the extra operating costs? In other words, when is it worth optimizing mixing? We address this question by characterizing the mixing performance of a family of optimal mixers in terms of the power input required to operate them, the computational cost involved in performing the optimizations and the total energy consumed to obtain a target homogenization level. We will present some unexpected and counter-intuitive results.

In § 2, we introduce the mathematical formulation of the Fourier sine flow, briefly describe the solution of the purely advective problem, discuss the procedure for the computation of the mix-norm and formulate the velocity profile optimization problem. In § 3, we evaluate the performance and costs of the four least computationally expensive mixers. In § 3.1, we study the effect of the velocity profile optimization alone by stirring the mixture with a periodic protocol. In § 3.2, we study the effect of coupling the velocity profile optimization with the simplest form of the short-time-horizon optimization. We conclude by summarizing our work and draw conclusions about the cost efficiency of the optimal mixers.

2. Mathematical formulation of the problem

In this section, we extend the sine flow in order to implement the velocity profile optimization. We briefly review the solution of the purely advective problem, summarize the computation of the mix-norm and formulate the velocity profile optimization problem.

2.1. *The Fourier sine flow*

The time-periodic sine flow (Liu *et al.* 1994) has been a popular playground for studying laminar mixing (Pierrehumbert 1994; Antonsen *et al.* 1996; Alvarez *et al.* 1998; Muzzio *et al.* 2000; Szalai *et al.* 2003; Thiffeault *et al.* 2004; Phelps & Tucker 2006). In the sine flow, a concentration field is stirred iteratively by a pair of orthogonal, sinusoidal velocity fields

$$\boldsymbol{u}_0(x, y) = U \sin\left(2\pi\frac{y}{L}\right)\hat{\boldsymbol{\imath}}, \quad \boldsymbol{u}_1(x, y) = U \sin\left(2\pi\frac{x}{L}\right)\hat{\boldsymbol{\jmath}}, \tag{2.1}$$

inside a square domain $\mathbb{V} = [0, L] \times [0, L]$ with periodic boundary conditions (see figure 1). The vectors $\hat{\boldsymbol{\imath}}$ and $\hat{\boldsymbol{\jmath}}$ are the unit vectors along the x and y axes, respectively, and U is the maximal amplitude of the stirring velocity field within the mixing domain $\mathbb{V}$. During each iteration, the concentration field is advected by only one of the two velocity fields, $\boldsymbol{u}_0$ or $\boldsymbol{u}_1$, over a switching time τ (see figure 1). A stirring protocol is defined as a sequence of N binary digits $\{\alpha_l\}_{l=1}^{N}$, where N is the total number of iterations to be performed. Entries α_l set to zero and one identify the velocity fields $\boldsymbol{u}_0$ and $\boldsymbol{u}_1$, respectively. The set of 2^N binary strings of length N represents all admissible protocols that can be used to stir the mixture by a given final time $T_h = \tau N$. The sine flow stirred by the periodic protocol $\{0, 1, 0, 1, \ldots\}$ is referred to as the time-periodic sine flow.

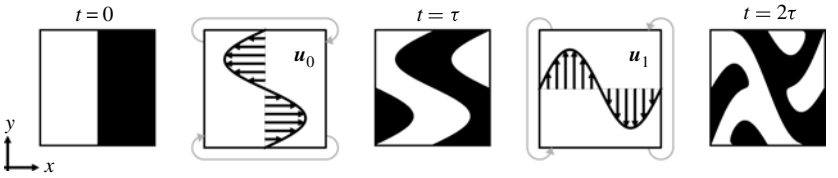

FIGURE 1. The schematic of the sine flow. The second and fourth panels visualize the stirring velocity fields $\boldsymbol{v}_0$ and $\boldsymbol{v}_1$, respectively, defined in (2.1). The curved arrows joining the opposite sides of the square mixing domain indicate periodic boundary conditions. The other panels depict the concentration field before and after the action of the stirring velocity fields.

To represent complex, periodic, zero-mean velocity profiles and allow for their optimization, we extend the velocity fields (2.1) using the Fourier representation

$$\left.\begin{aligned} \boldsymbol{v}_0(x,y) &= U\sum_{k=1}^{\infty} a_k \sin\left[2\pi\left(k\frac{y}{L}+p_k\right)\right]\hat{\boldsymbol{\imath}},\\ \boldsymbol{v}_1(x,y) &= U\sum_{k=1}^{\infty} a_k \sin\left[2\pi\left(k\frac{x}{L}+p_k\right)\right]\hat{\boldsymbol{\jmath}}, \end{aligned}\right\} \tag{2.2}$$

where k, a_k and p_k are the wavenumber, amplitude and phase shift of the kth Fourier mode, respectively. Note that these coefficients are dimensionless, and, since the velocity fields never act together, we use the same symbols, k, a_k and p_k, for both velocity fields to simplify notation. We call our extension (2.2) the *Fourier sine flow*. We refer to the Fourier mode with the lowest wavenumber, $k = 1$, as the fundamental mode. The sine flow (2.1) can be recovered from the Fourier sine flow (2.2) by setting all amplitudes but the fundamental to zero, and setting the amplitude and phase shift of the fundamental mode to one and zero, respectively.

In this study, we want to compare the mixing performance and the cost efficiency of mixers that optimize the profile of the stirring velocity fields by using different numbers of Fourier modes, and, for each mode, different amplitudes and phase shifts. To this end, we must adimensionalize the Fourier sine flow using a characteristic length and time that are independent of the number of modes, and their amplitudes and phase shifts. Furthermore, to enable a comparison of our present results with the existing results obtained for the sine flow, we must ensure that the characteristic quantities of the Fourier sine flow are the same as the characteristic quantities of the sine flow. In the sine flow, the characteristic length equals the side of the mixing domain, L. The characteristic time, instead, if molecular diffusion is negligible, is the characteristic advection time, which is equal to the ratio of L over the maximal magnitude of the stirring velocity field, U. Naturally, we choose the side of the domain, L, as the characteristic length for the Fourier sine flow. The choice of the characteristic velocity and, consequently, of the characteristic advection time is less obvious. In fact, in the case of a velocity profile synthesized by multiple Fourier modes, the maximal magnitude of the velocity depends on the amplitudes and phase shifts of the modes. This dependence must be avoided to allow for a correct optimization of the modes and a fair comparison between different flow configurations. Hence, we choose as a characteristic velocity of the Fourier sine flow a velocity

proportional to the root mean square (r.m.s.) of the stirring velocity field, i.e.

$$U' = U_{rms}\sqrt{2} = \sqrt{\frac{2}{L}\int_0^L \boldsymbol{v}_0 \cdot \boldsymbol{v}_0 \,\mathrm{d}y} = \sqrt{\frac{2}{L}\int_0^L \boldsymbol{v}_1 \cdot \boldsymbol{v}_1 \,\mathrm{d}x} = U\sum_{k=1}^{\infty} a_k^2, \tag{2.3}$$

where U_{rms} is the r.m.s. velocity. The coefficient $\sqrt{2}$ in (2.3) is included so that U' is equal to U in the case of sine flow, i.e. when $a_1 = 1$ is the only non-zero amplitude. To enable a fair comparison between the sine and Fourier sine flow, we impose that $U' = U$, i.e.

$$\sum_{k=1}^{\infty} a_k^2 = 1. \tag{2.4}$$

This constraint on the amplitudes of the Fourier modes can also be interpreted as a constraint on the kinetic energy per unit mass of the stirring flow, under the assumption that the fluids to be mixed have equal and constant density.

It is important to note that mixers that satisfy the above constraint alone cannot be fairly compared because they can produce different amounts of shear stress within the mixture. In general, higher amounts of shear stress induce more efficient stretching of fluid elements, which results in higher mixing performance. Therefore, without a constraint limiting the amount of shear stress produced, the optimization routine always assigns the highest possible amplitude to the highest-frequency mode. This optimization strategy is unrealistic in physically realizable mixing devices because an increase in shear stress implies an increase of the energy dissipated by a fluid due to viscosity (Khakhar, Rising & Ottino 1986; Ottino 1989; Vikhansky 2002*b*). In turn, this increase in the dissipated energy requires higher power input to operate the mixing device. Consequently, to obtain a realistic velocity profile optimization problem, we define and constrain the power input needed to operate our conceptual mixer.

The power input can be defined as the rate at which the actuating system does work to stir the mixture contained within the domain $\mathbb{V}$. It can be expressed as

$$P_{in} = \frac{\mathrm{d}}{\mathrm{d}t}\int_{\mathbb{V}} \frac{1}{2}\rho \boldsymbol{v}\cdot\boldsymbol{v}\,\mathrm{d}V + \int_{\mathbb{V}} \boldsymbol{\sigma} : \boldsymbol{D}\,\mathrm{d}V, \tag{2.5}$$

where ρ is the fluid density, $\boldsymbol{v}$ is the fluid velocity, $\boldsymbol{\sigma}$ is the stress tensor and $\boldsymbol{D} = [\boldsymbol{\nabla v} + (\boldsymbol{\nabla v})^{\mathrm{T}}]/2$ is the stretching tensor (Malvern 1969). The superscript 'T' indicates transpose. Equation (2.5) states that the power input contributes to the kinetic energy of the fluids, through the first term on the right-hand side, and to internal energy of the fluids, through the second term, respectively. In laminar flow regimes, the regimes considered in this study, the second term dominates, and the power input can be approximated by this term only (Bigio & Conner 1995; Lamberto, Alvarez & Muzzio 2001). In the case of incompressible, Newtonian fluids, the power input per unit mass of the Fourier sine flow (2.2) is

$$P_{in}(\boldsymbol{v}_0) = P_{in}(\boldsymbol{v}_1) = 2\pi^2\nu\frac{U^2}{L^2}\sum_{k=1}^{\infty}(ka_k)^2, \tag{2.6}$$

where ν is the kinematic viscosity, which, for simplicity, we assume to be constant and equal for all fluids to be mixed. Hence, we conclude that two flows can be fairly compared and correctly optimized only when they have the same power input per unit mass.

We adimensionalize the Fourier sine flow using L as a characteristic length and the characteristic advection time $T = L/U = L/U'$ as a characteristic time. We define the dimensionless switching time, $\tilde{\tau} = \tau/T$, the dimensionless final time or homogenization time, $\tilde{T}_h = T_h/T$, the dimensionless coordinates, $\tilde{x} = x/L$ and $\tilde{y} = y/L$, and the dimensionless velocity fields, $\tilde{\boldsymbol{v}}_0 = \boldsymbol{v}_0/U$ and $\tilde{\boldsymbol{v}}_1 = \boldsymbol{v}_1/U$. We define the characteristic power input per unit mass of the Fourier sine flow as $P = 2\pi^2\nu U^2/L^2$, i.e. as the power input of the time-periodic sine flow. Hence, the dimensionless power input per unit mass is $\tilde{P}_{in} = P_{in}/P$.

To simplify notation we drop the tildes, with the understanding that all variables and equations are dimensionless hereafter. Hence, the dimensionless Fourier sine flow iteratively stirs a mixture on a unit square domain by a pair of orthogonal velocity fields

$$\boldsymbol{v}_0(x, y) = \sum_{k=1}^{\infty} a_k \sin[2\pi(ky + p_k)]\hat{\boldsymbol{\imath}}, \quad \boldsymbol{v}_1(x, y) = \sum_{k=1}^{\infty} a_k \sin[2\pi(kx + p_k)]\hat{\boldsymbol{\jmath}}, \tag{2.7}$$

having unit kinetic energy and power input

$$P_{in} = \sum_{k=1}^{\infty} (ka_k)^2 . \tag{2.8}$$

Note that the sine flow is the only flow that has unit kinetic energy and unit power input because, in this case, $a_1 = 1$ is the only non-zero amplitude. Once the higher-order modes are engaged, i.e. when $a_k \neq 0$ for $1 \leqslant k \leqslant H$, where H is the number of Fourier modes used to synthesize the profile of the stirring velocity field, the power input of the Fourier sine flow has to be higher than the power input of the sine flow. It follows that the choice of the power input determines, among all possible mixers, which mixers can be compared and then optimized. Note that the sine flow cannot be fairly compared with any Fourier sine flow, but it provides a useful benchmark to characterize the mixing performance and cost efficiency of the Fourier sine flow.

The power input constraint (2.8) and the kinetic energy constraint (2.4) are equally crucial for a meaningful and realistic optimization of the velocity profiles. Without (2.8), for a fixed value of the kinetic energy, the mixing performance can be unboundedly increased by choosing Fourier modes of higher and higher frequency, i.e. unboundedly increasing the power input. Without (2.4), for a fixed value of the power input, choosing higher and higher frequency modes unboundedly decreases the kinetic energy to zero while increasing the mixing efficiency. In this study, therefore, we enforce both constraints simultaneously.

2.2. *Solution of the purely advective problem*

The advection of a concentration field $\varphi(x, y, t)$ due to the stirring action of the velocity field $\boldsymbol{v}_{\alpha_l}$ is governed by the equation

$$\frac{\partial \varphi}{\partial t} = -\boldsymbol{v}_{\alpha_l} \cdot \boldsymbol{\nabla}\varphi, \tag{2.9}$$

where $l = 1, 2, \ldots, N$, the iteration number, controls the time evolution of the system, i.e. $(l-1)\tau \leqslant t < l\tau$, and the velocity field $\boldsymbol{v}_{\alpha_l}$ is either $\boldsymbol{v}_0$ if α_l is zero, or $\boldsymbol{v}_1$ if α_l is one (see figure 1). The above equation is to be solved within a unit square domain equipped with periodic boundary conditions for a given initial concentration field $\varphi_0 = \varphi(x, y, 0)$.

Equation (2.9) states that the concentration associated with any fluid particle is preserved in time. Hence, the time evolution of the concentration field can be obtained from the time evolution of the fluid particles moving under the action of the stirring velocity fields (2.7). To compute the evolution of the concentration field, we discretize the unit square domain into $M \times M$ non-overlapping equal square cells, where M, the *grid resolution*, is an integer number. The concentration within the (i, j)th cell is approximated by the concentration of the fluid particle $(X_l^{i,j}, Y_l^{i,j})$ located at time $t = l\tau$ at the centre of the cell. The position of this particle is tracked backwards in time to the initial position $(X_0^{i,j}, Y_0^{i,j})$ using the map

$$\begin{pmatrix} X_{m-1}^{i,j} \\ Y_{m-1}^{i,j} \end{pmatrix} = \begin{cases} \begin{pmatrix} X_m^{i,j} - \tau \displaystyle\sum_{k=1}^{\infty} a_k \sin[2\pi(kY_m^{i,j} + p_k)] \\ Y_m^{i,j} \end{pmatrix} \bmod 1 & \text{if } \alpha_m = 0, \\ \begin{pmatrix} X_m^{i,j} \\ Y_m^{i,j} - \tau \displaystyle\sum_{k=1}^{\infty} a_k \sin[2\pi(kX_m^{i,j} + p_k)] \end{pmatrix} \bmod 1 & \text{if } \alpha_m = 1, \end{cases} \tag{2.10}$$

for $m = l, l-1, l-2, \ldots, 1$. Then, the concentration associated with the (i, j)th particle at time $t = l\tau$ is

$$\varphi(X_l^{i,j}, Y_l^{i,j}, t_k) = \varphi(X_0^{i,j}, Y_0^{i,j}, 0). \tag{2.11}$$

2.3. *Computation of the mix-norm*

In this study, the mix-norm is used as a diagnostic to quantify the performance of our mixing device as well as a cost function to optimize the velocity profiles and the stirring protocol. Consequently, it is important to compute the mix-norm efficiently and accurately.

The mix-norm is a multi-scale measure of the mixedness of a concentration field. It was introduced by Mathew *et al.* (2005) and is defined as the r.m.s. of the average values of the concentration field over a dense set of subsets contained in the flow domain. In the case of a square domain with periodic boundaries, the mix-norm μ_φ of a concentration field $\varphi(x, y, t)$ having zero mean can be written as (Mathew *et al.* 2005)

$$\mu_\varphi = \sqrt{\sum_{m,n\in\mathbb{Z}} \frac{|\Phi_{m,n}|^2}{\sqrt{1 + 4\pi^2(m^2 + n^2)}}}, \tag{2.12}$$

where $\{\Phi_{m,n}\}_{m,n\in\mathbb{Z}}$ is the spectral representation of the concentration field. In the case when the mean concentration is not zero, the mix-norm can still be used provided that the mean value is subtracted from the concentration field before computing its spectral representation.

An approximate spectral representation of the concentration field $\varphi(x, y, t)$ can be obtained by computing the fast Fourier transform (FFT) of its discrete representation $\varphi(X_l^{i,j}, Y_l^{i,j})$ at time $t = l\tau$, where $i, j = 1, \ldots, M$. The mix-norm is then obtained by substituting the Fourier coefficients $\Phi_{m,n}$ into (2.12). To ensure that the value of the mix-norm computed in the purely advective case is sufficiently accurate and, at the same time, the computation is practically feasible, we use the grid

resolution $M = 2048$. The validity of this resolution is discussed in detail by Gubanov & Cortelezzi (2009).

2.4. *Formulation of the velocity profile optimization problem*

We implement the optimization of the velocity profile of the Fourier sine flow (2.7) as follows. Starting at $t = 0$, we first compute up to $t = \tau$ the solution to the problem (2.9) for a given value of the a_k and p_k with initial condition $\varphi(x, y, 0)$. Then, we derive its spectral representation and substitute it into (2.12) to evaluate the mix-norm, our cost function. Numerical experiments indicate that the cost function is smooth in the a_k and p_k. Therefore, we solve the optimization problem of minimizing the mix-norm using a conventional gradient-based optimization method and compute the optimal amplitudes, a_k, and phase shifts, p_k. We repeat the procedure and evolve the concentration field using the optimal solution $\varphi(x, y, \tau)$ as an initial condition for the next iteration, $\tau \leqslant t \leqslant 2\tau$, and so on until the desired level of homogenization is reached.

The computational cost of this optimization can be substantially reduced by choosing appropriate ranges for the a_k and p_k. The feasible range for p_k, for all $k \geqslant 1$, is the interval $[0, 1]$ because the kth mode is periodic in p_k with period of unity. The feasible range for a_k, for all $k \geqslant 1$, is bounded by the kinetic energy constraint (2.4), which implies that $|a_k| \leqslant 1$ for all $k \geqslant 1$. Note that the range for a_k, for all $k \geqslant 1$, can be further restricted to the interval $[0, 1]$ because a mode with a negative amplitude a_k is equivalent to a mode with a positive amplitude $a_k' = -a_k$ and phase shift $p_k' = (p_k + 1/2) \bmod 1$.

In order to solve the velocity profile optimization problem numerically, we truncate the Fourier series in (2.7) to its first H modes. In other words, we consider the optimization of velocity profiles that are the synthesis of a finite number of modes. Then, the problem of finding the optimal amplitudes and phase shifts of these modes that minimize the mix-norm can be formulated as follows:

$$\min_{a_1,a_2,\ldots,a_H,\, p_1,p_2,\ldots,p_H} \mu_\varphi(a_1, a_2, \ldots, a_H, p_1, p_2, \ldots, p_H)\big|_{t=l\tau}, \quad l = 1, 2, \ldots, \tag{2.13}$$

subject to $2H$ bounds constraints

$$0 \leqslant a_k \leqslant 1, \quad 0 \leqslant p_k \leqslant 1, \quad k = 1, 2, \ldots, H, \tag{2.14}$$

and two equality constraints

$$\sum_{k=1}^{H} a_k^2 = 1, \tag{2.15}$$

$$\sum_{k=1}^{H} (ka_k)^2 = P_{in}. \tag{2.16}$$

Note that the above optimization problem has a solution only when $1 \leqslant P_{in} \leqslant H^2$. It is easy to show that the sum on the left-hand side of (2.16) reaches its minimum when $a_1 = 1$ and $a_2 = a_3 = \cdots = a_H = 0$, and its maximum when $a_H = 1$ and $a_1 = a_2 = \cdots = a_{H-1} = 0$.

We compute the optimal amplitudes and phase shifts by minimizing the mix-norm using the derivative-free pattern search method (see Lewis & Torczon 2000, and references therein), which is implemented in the APPSPACK library (see Kolda 2005, and references therein). Note that this library solves only optimization problems with linear constraints, whereas the constraints to our optimization problem, (2.15)

and (2.16), are nonlinear. To overcome this difficulty, in the numerical implementation of the problem, we replace the optimization variables a_k, $k \geqslant 1$, with the variables $\hat{a}_k = \sqrt{a_k}$, for all $k \geqslant 1$, and obtain constraints that are linear in $\hat{a}_k$. However, for the sake of clarity, we formulate constraints in terms of a_k throughout this study.

The optimization problem (2.13)–(2.16) becomes particularly simple when $H = 1$. In this case, the feasible value of the power input is unique, $P_{in} = 1$, which implies $a_1 = 1$. The phase shift p_1 is the only optimization variable. Thus, when $H = 1$, the Fourier sine flow is equivalent to the sine flow in which the stirring velocity fields are shifted along the associate coordinate axis by an intelligently chosen phase at each iteration of the periodic protocol. Gubanov & Cortelezzi (2010) showed that this mixer is nearly insensitive to the geometry of the initial concentration field because the optimization of the phase p_1 intelligently controls the spatial distribution of stretching within the mixing domain.

In the present study we consider higher values of H, namely $H = 2$, 3 and 4, in order to synthesize more effective velocity profiles and use $H = 1$ as a reference case. In the case $H = 2$, the constraints (2.15) and (2.16) restrict the feasible amplitudes to a single pair

$$a_1 = \sqrt{(4 - P_{in})/3}, \quad a_2 = \sqrt{(P_{in} - 1)/3}, \tag{2.17}$$

where the power input $P_{in} \in [1, 4]$. Hence, the optimization problem reduces to the selection of the optimal phases p_1 and p_2 that minimize the mix-norm, i.e.

$$\min_{0 \leqslant p_1, p_2 \leqslant 1} \mu_\varphi(p_1, p_2)\big|_{t = l\tau}, \quad l = 1, 2, \ldots, \tag{2.18}$$

and is solved numerically using a pattern search method implemented in APPSPACK. Note that the pattern search is a local optimization method, which only guarantees convergence to a local minimum. To increase the chance of finding the global minimum, we perform four local optimizations starting from four initial guesses that uniformly cover the feasible domain, i.e. $p_1 = j_1/3$, $p_2 = j_2/3$ for j_1, $j_2 = 1, 2$. The best of the four solutions is chosen as a reasonable approximation to the global solution.

In the case $H = 3$, the power input P_{in} belongs to the interval $[1, 9]$, and the feasible range of amplitude a_1 is $[a_1^{min_3}, a_1^{max_3}]$, where

$$a_1^{min_3} = \begin{cases} 0 & \text{if } P_{in} \geqslant 4, \\ \sqrt{(4 - P_{in})/3} & \text{if } P_{in} < 4, \end{cases} \qquad a_1^{max_3} = \sqrt{(9 - P_{in})/3}. \tag{2.19}$$

Having chosen a value for the power input P_{in} and an amplitude a_1, the amplitudes a_2 and a_3 are uniquely determined as

$$a_2 = \sqrt{(9 - P_{in} - 8a_1^2)/5}, \quad a_3 = \sqrt{(P_{in} - 4 + 3a_1^2)/5}. \tag{2.20}$$

The optimization problem reduces to the selection of the optimal amplitude a_1 and the optimal phases p_1, p_2 and p_3 that minimize the mix-norm, i.e.

$$\min_{\substack{0 \leqslant p_1, p_2, p_3 \leqslant 1, \\ a_1^{min_3} \leqslant a_1 \leqslant a_1^{max_3}}} \mu_\varphi(a_1, p_1, p_2, p_3)\big|_{t = l\tau}, \quad l = 1, 2, \ldots. \tag{2.21}$$

This problem is solved numerically using the same pattern search method as used in the case $H = 2$. In this case, however, the global solution is approximated by choosing

the best of 16 local solutions obtained by starting the pattern search method from 16 initial guesses uniformly distributed over the feasible domain, i.e. $p_1 = j_1/3$, $p_2 = j_2/3$, $p_3 = j_3/3$, $a_1 = a_1^{min_3} + j_4(a_1^{max_3} - a_1^{min_3})/3$ for $j_k = 1, 2$, $k = 1, 2, 3, 4$.

The complexity of the optimization problem grows quickly with H. In the case $H = 4$, the power input P_{in} belongs to the interval $[1, 16]$, and the feasible range of a_1 is $[a_1^{min_4}, a_1^{max_4}]$, where

$$a_1^{min_4} = a_1^{min_3}, \quad a_1^{max_4} = \sqrt{(16 - P_{in})/15}. \tag{2.22}$$

Given a value for the power input P_{in} and the amplitude a_1, the feasible range of the amplitude a_2 is $[a_2^{min_4}, a_2^{max_4}]$, where

$$a_2^{min_4} = \begin{cases} 0 & \text{if } P_{in} \geqslant 9 - 8a_1^2, \\ \sqrt{(9 - P_{in} - 8a_1^2)/5} & \text{if } P_{in} < 9 - 8a_1^2, \end{cases} \tag{2.23}$$

and

$$a_2^{max_4} = \begin{cases} 0 & \text{if } P_{in} \geqslant 16 - 15a_1^2, \\ \sqrt{(16 - P_{in} - 15a_1^2)/12} & \text{if } P_{in} < 16 - 15a_1^2. \end{cases} \tag{2.24}$$

Having chosen the values of $P_{in} \in [1, 16]$, $a_1 \in [a_1^{min_4}, a_1^{max_4}]$ and $a_2 \in [a_2^{min_4}, a_2^{max_4}]$, the amplitudes a_3 and a_4 are uniquely determined as

$$a_3 = \sqrt{(16 - P_{in} - 15a_1^2 - 12a_2^2)/7}, \quad a_4 = \sqrt{(P_{in} - 9 + 8a_1^2 + 5a_2^2)/7}. \tag{2.25}$$

Hence, the optimization problem reduces to the selection of the optimal amplitudes a_1 and a_2 and the optimal phases p_1, p_2, p_3 and p_4 that minimize the mix-norm, i.e.

$$\min_{\substack{0 \leqslant p_1, p_2, p_3, p_4 \leqslant 1, \\ a_1^{min_4} \leqslant a_1 \leqslant a_1^{max_4}, \\ a_2^{min_4} \leqslant a_2 \leqslant a_2^{max_4}}} \mu_\varphi(a_1, a_2, p_1, p_2, p_3, p_4)\big|_{t = l\tau}, \quad l = 1, 2, \ldots. \tag{2.26}$$

To solve the problem (2.26), the pattern search method is started from 64 initial guesses uniformly distributed over the feasible domain, i.e. $p_1 = j_1/3$, $p_2 = j_2/3$, $p_3 = j_3/3$, $p_4 = j_4/3$, $a_1 = a_1^{min_4} + j_5(a_1^{max_4} - a_1^{min_4})/3$, $a_2 = a_2^{min_4} + j_6(a_2^{max_4} - a_2^{min_4})/3$ for $j_k = 1, 2$, $k = 1, 2, 3, 4, 5, 6$. Optimization problems involving more than four modes become prohibitively complicated and computationally expensive.

3. Mixing performance and operating cost of the mixers M_H^α

Having selected a number of modes, $H \geqslant 1$, and a stirring protocol, α, we represent with the symbol M_H^α a mixer that stirs the Fourier sine flow with a protocol α and velocity fields whose profiles are the solutions to the optimization problem (2.13)–(2.16). In this section, we characterize the cost and efficiency of the four least computationally expensive mixers, M_1^α, M_2^α, M_3^α and M_4^α, or $M_{1,2,3,4}^\alpha$ in a more compact notation.

The mixer M_1^α (Gubanov & Cortelezzi 2010) involves the simplest form of velocity profile optimization. In this case, the sinusoidal velocity profiles are shifted by an optimal phase p_1 along the corresponding coordinate axis at each iteration of the protocol. Since the mixer M_1^α will be used throughout this article as a benchmark, we briefly recall our previous results. We defined an appropriate operating range of

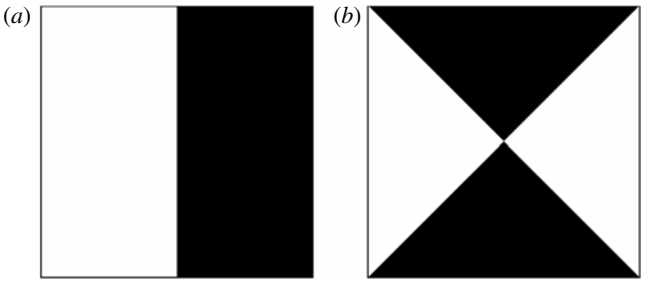

FIGURE 2. The (*a*) 'vertical' and (*b*) 'envelope' initial configurations of the concentration field. The initial concentration $\varphi(x, y, 0)$ is equal to -1 and $+1$ inside the black and white regions, respectively.

switching times, $0.1 \leqslant \tau \leqslant 1.3$, and a target mixing performance, i.e. a desired level of homogenization $\mu_\varphi(T_h) = 0.03$, to be achieved by a final time $T_h = 6$. We showed that the mixer M_1^{per}, where the superscript *per* identifies the periodic protocol, achieves the target performance over a range of medium to high switching times, $0.5 \leqslant \tau \leqslant 1.3$, and is nearly insensitive to the geometry of the initial configuration of the mixture. We observed, however, that, for low switching times, $0.1 \leqslant \tau \leqslant 0.4$, the mixer M_1^{per} is unable to obtain the desired level of homogenization. To overcome this difficulty, we coupled the phase optimization with the optimization of the stirring protocol. We implemented, at each iteration of the sine flow, the following two-step procedure. First, the optimal phases for both stirring velocity fields $\boldsymbol{v}_0$ and $\boldsymbol{v}_1$ were computed. Second, the best performing of the two optimal velocity fields was selected. We named *optimal* the mixer that implements this coupled optimization strategy because it delivers the target performance over the entire range of switching times, and is nearly insensitive to the initial geometrical configuration of the mixture. Here we identify the optimal mixer as M_1^{opt}.

In this study, we extend our previous work by addressing the problem of designing optimal mixers that minimize the time and cost of achieving a desired level of homogenization. We choose as the target level of homogenization the mix-norm value $\mu_h = 0.03$, i.e. the value obtained by the mixer M_1^{opt} by the time $T_h = 6$. Using M_1^{α} as a benchmark, we characterize the mixing performance and the operating cost of the mixers $M_{2,3,4}^{\alpha}$ by analysing different cost functions: the homogenization time T_h needed to achieve the desired level of homogenization, the computational cost C needed to obtain an optimal sequence of stirring velocity fields, and the total energy consumption $E_{in} = P_{in}T_h$, i.e. the energy required to operate the mixer to obtain the target level of homogenization.

We assume that the homogenization time T_h, the computational cost C and the total energy consumption E_{in} depend on five parameters: the number of modes, H, used to synthesize the stirring velocity profiles; the type of stirring protocol, α; the power input, P_{in}; the switching time, τ; and the initial configuration of the mixture, φ_0. We explore this parameter space by choosing for each parameter a number of representative values. The chosen values sample the parameter space reasonably well and, at the same time, their number is sufficiently small to make the computation of T_h feasible. We choose $H = \{2, 3, 4\}$ and $\alpha = \{per, opt\}$. The choice of H implies that P_{in} belongs to the range $1.0 \leqslant P_{in} \leqslant 4.0$, the common range of feasible power inputs for mixers $M_{2,3,4}^{\alpha}$. We sample this range uniformly with the values $P_{in} = 1.0,\ 1.1,\ 1.2, \ldots, 3.9,\ 4.0$. As initial configurations of the concentration

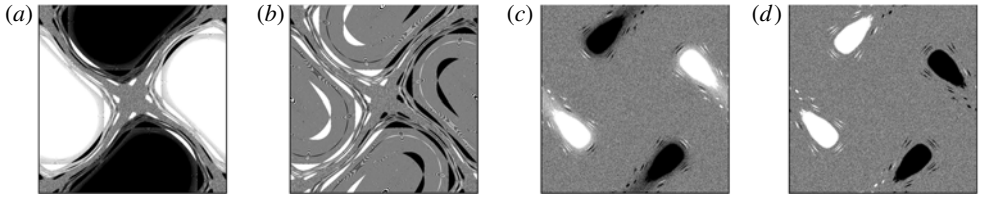

FIGURE 3. Snapshots at time $t = 600$ of the concentration field φ stirred by the sine flow operating at switching times (a,b) $\tau = 0.2$ and (c,d) $\tau = 0.4$ when applied to the (a,c) 'envelope' and (b,d) 'vertical' initial configuration.

field, φ_0, we use the 'vertical' and 'envelope' initial configurations shown in figure 2. These two configurations have been shown to be the easiest and hardest to mix by the sine flow, respectively (Gubanov & Cortelezzi 2009). We indicate the 'vertical' and 'envelope' initial configurations as $\varphi_0 = V$ and $\varphi_0 = E$, respectively.

The test values for τ are chosen based on the performance of the mixer M_1^{α}. Within the range of low to moderate switching times, $0.1 \leqslant \tau \leqslant 0.5$, the mixer M_1^{per} is known to perform poorly with respect to the mixer M_1^{opt} (Gubanov & Cortelezzi 2010). For higher switching times, the two mixers deliver nearly the same, optimal performance. Therefore, we focus our study on the range $0.1 \leqslant \tau \leqslant 0.5$ and select $\tau = 0.2$ and 0.4 as the representative values. The challenge of operating at these switching time values is clearly exemplified by the sine flow. Figure 3 shows the snapshots of the concentration fields stirred by the sine flow at time $t = 600$, i.e. after 3000 iterations for $\tau = 0.2$ and 1500 iterations for $\tau = 0.4$, respectively. By this time, the sine flow is still far from reaching the target homogenization level $\mu_h = 0.03$. The values of the mix-norm, $\mu_\varphi = 0.3$ (figure 3*a*) and 0.1 (figure 3*c*), show that the 'envelope' initial concentration field is especially hard to mix with respect to the 'vertical' initial configuration, $\mu_\varphi = 0.06$ (figure 3*b*) and 0.08 (figure 3*d*). This poor performance is due to the persistence of the islands of regular motion induced by the periodic protocol.

3.1. *Mixers equipped with velocity profile optimization and periodic stirring protocol*

It is of interest to characterize the efficiency of the velocity profile optimization alone because one can hope to produce optimal mixers without the need to couple this optimization with the stirring protocol optimization. To perform this characterization, we compute the homogenization time T_h needed by the mixers $M_{2,3,4}^{per}$ to generate a mixture of the desired homogenization value, or mix-norm value, $\mu_h = 0.03$, using a periodic stirring protocol. Figure 4 shows the values of T_h versus the power input P_{in} at which the mixers operate. Circles, triangles and squares indicate mixers M_2^{per}, M_3^{per} and M_4^{per}, respectively. Black and dark-grey symbols correspond to the 'vertical' initial configuration and indicate switching times $\tau = 0.2$ and 0.4, respectively. White and light-grey symbols correspond to the 'envelope' initial configuration and indicate switching times $\tau = 0.2$ and 0.4, respectively. Note that all mixers are able to achieve the target homogenization value at most by time $t = 10$. This is a striking improvement in performance with respect to the sine flow, which is unable to produce the target homogenization level by time $t = 600$ (see figure 3).

In figure 4, the values of the homogenization time T_h corresponding to $P_{in} = 1$ represent the performance of the mixer M_1^{per} (Gubanov & Cortelezzi 2010). Note that at $P_{in} = 1$ the mixers M_H^{per}, for all $H > 1$, perform exactly as mixer M_1^{per} because, for this value of power input, only the fundamental mode can be used. Note that we

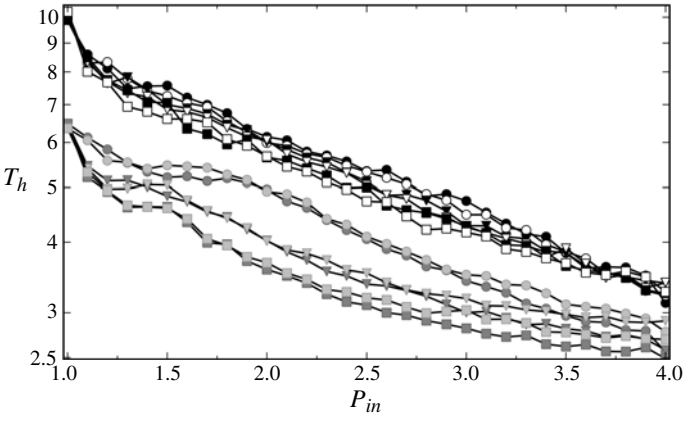

FIGURE 4. Time T_h needed for obtaining the target homogenization value $\mu_h = 0.03$ by mixers M_2^{per} (circles), M_3^{per} (triangles) and M_4^{per} (squares) versus power input P_{in}. Black and white symbols correspond to $\tau = 0.2$ and indicate cases $\varphi_0 = V$ and $\varphi_0 = E$, respectively. Dark- and light-grey symbols correspond to $\tau = 0.4$ and indicate cases $\varphi_0 = V$ and $\varphi_0 = E$, respectively. The homogenization times induced by the mixer M_1^{per} are shown at $P_{in} = 1.0$.

observe different values of T_h at $P_{in} = 1$ because the homogenization time depends on the switching time, τ, used and the initial configuration, φ_0, selected. Figure 4 shows that, for any given combination of τ and φ_0, the homogenization time obtained for $P_{in} = 1$ is higher than the homogenization times obtained for any other power input. Therefore, mixers $M_{2,3,4}^{per}$ always perform equally to or better than M_1^{per}, consistently with the fact that $M_{2,3,4}^{per}$ operate at power input equal to or higher than M_1^{per}.

Figure 4 shows that, for $P_{in} = 1$ and $\tau = 0.4$, the desired level of homogenization is obtained about 1.5 times faster than for $P_{in} = 1$ and $\tau = 0.2$. This difference remains visible for all values of power input considered, resulting in two clearly separated groups of curves: the upper group that corresponds to $\tau = 0.2$, and the lower group that corresponds to $\tau = 0.4$. Furthermore, the curves within the upper group are tightly packed together, indicating that for $\tau = 0.2$ the more computationally expensive mixers, $M_{3,4}^{per}$, have a mixing performance only marginally better than the performance of M_2^{per}. The homogenization times of the two groups of curves indicate that the velocity profile optimization is more effective for $\tau = 0.4$ than for $\tau = 0.2$. These differences preclude assessing the cost efficiency of the mixers $M_{2,3,4}^{per}$ uniformly with respect to the switching time τ, and indicate that it is impossible to design an optimal mixer relying on the velocity profile optimization alone.

The poor mixing performance of the mixers $M_{1,2,3,4}^{per}$ operating at switching time $\tau = 0.2$ is captured by the snapshots of the concentration field shown in figure 5. These snapshots correspond to the mix-norm value of about $\mu_\varphi = 0.06$, twice the target homogenization level μ_h. The snapshots present intricately folded, irregularly distributed striations whose thickness varies considerably over the mixing domain. The intricacy of folding tends to increase when increasing the power input and the number of Fourier modes; see figure 5(*a–e*). The presence of relatively thick striations even for high power inputs indicates a lack of stretching. Owing to the periodicity of the protocol, the mixers $M_{1,2,3,4}^{per}$ are unable to generate sufficient stretching and, consequently, compensate for this deficiency with excessive folding.

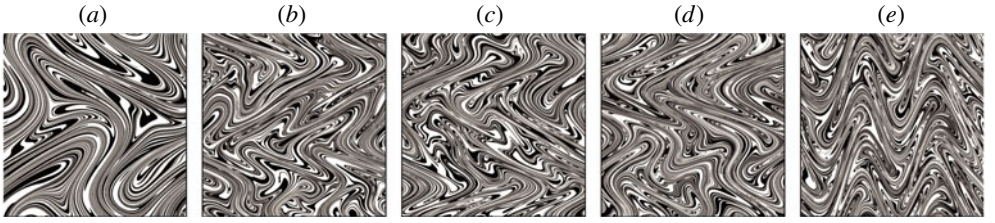

FIGURE 5. Snapshots at times (*a*) 6.2, (*b*) 4.2, (*c*,*d*) 3.8 and (*e*) 2.8 of the concentration field φ stirred by mixers (*a*) M_1^{per}, (*b*,*e*) M_3^{per}, (*c*) M_4^{per} and (*d*) M_2^{per} operating at switching time $\tau = 0.2$ and power inputs (*a*) P_{in}=1.0, (*b*,*c*) 2.0, (*d*) 2.5 and (*e*) 3.5 when applied to the (*a*,*b*,*d*) 'vertical' and (*c*,*e*) 'envelope' initial configuration.

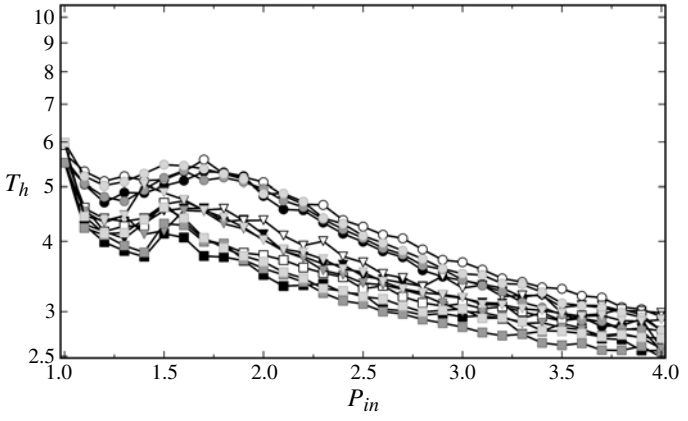

FIGURE 6. Value of the homogenization time T_h achieved by mixers M_2^{opt} (circles), M_3^{opt} (triangles) and M_4^{opt} (squares) versus power input P_{in}. Black and white symbols correspond to $\tau = 0.2$ and indicate cases $\varphi_0 = V$ and $\varphi_0 = E$, respectively. Dark- and light-grey symbols correspond to $\tau = 0.4$ and indicate cases $\varphi_0 = V$ and $\varphi_0 = E$, respectively. The homogenization times induced by the mixer M_1^{opt} are shown at $P_{in} = 1.0$.

3.2. *Mixers equipped with coupled velocity profile and stirring protocol optimizations*

In this subsection we discuss the performance of a family of optimal mixers, M_2^{opt}, M_3^{opt} and M_4^{opt}, obtained by coupling the velocity profile optimization with the optimization of the stirring protocol. To characterize their cost efficiency, we compute the homogenization time T_h needed by the mixers $M_{2,3,4}^{opt}$ to generate a mixture that has the desired homogenization level, $\mu_h = 0.03$, versus the power input P_{in} needed to operate the mixers (see figure 6). Circles, triangles and squares indicate mixers M_2^{opt}, M_3^{opt} and M_4^{opt}, respectively. Black and dark-grey symbols correspond to the 'vertical' initial configuration. White and light-grey symbols correspond to the 'envelope' initial configuration. Black and white symbols indicate switching time $\tau = 0.2$. Dark- and light-grey symbols indicate switching time $\tau = 0.4$. In figure 6, the values of the homogenization time T_h corresponding to $P_{in} = 1$ represent the performance of the optimal mixer M_1^{opt} (Gubanov & Cortelezzi 2010). These values represent a benchmark for the performance of the mixers $M_{2,3,4}^{opt}$ because, at $P_{in} = 1$, the mixers $M_{2,3,4}^{opt}$ perform exactly as M_1^{opt} since only the fundamental mode can be used for this value of power input. For power inputs greater than unity, the mixers $M_{2,3,4}^{opt}$ always perform better

than M_1^{opt}, for all switching times and initial configurations, except for one case where the performance is the same.

The beneficial effect of coupling the velocity profile optimization with the optimization of the stirring protocol can be seen by comparing figure 6 to figure 4, which present, on the same scale, the homogenization time T_h versus power input P_{in}. Figure 6 shows that the curves for the switching time $\tau = 0.2$ collapse onto the better-performing curves for $\tau = 0.4$, forming three distinct groups of curves, one for each mixer. The remarkable reduction in homogenization time obtained by the mixers $M_{2,3,4}^{opt}$ operating at $\tau = 0.2$ is due to the stirring protocol optimization, which produces the optimal amount of stretching by prescribing the velocity fields $\boldsymbol{v}_0$ or $\boldsymbol{v}_1$ over several consecutive iterations.

In figure 6, the collapse of all curves into three distinct groups suggests that, unlike in the periodic case (see figure 4), the homogenization times generated by the mixers $M_{2,3,4}^{opt}$ are nearly independent of the switching time τ and the initial configuration of the mixture. We verified this result for several values of the switching time τ in the range $0.1 \leqslant \tau \leqslant 0.6$. Therefore, coupling the velocity profile and stirring protocol optimizations is essential for achieving a uniform mixing performance over a wide range of switching times and initial configurations, even when a higher number of modes are considered. This observation extends the results obtained for the optimal mixer M_1^{opt} (Gubanov & Cortelezzi 2010) to the mixers M_H^{opt}, $H > 1$, which are hence optimal.

A further comparison of figures 4 and 6 shows that, unlike in the periodic case, the homogenization time T_h achieved by the mixers $M_{2,3,4}^{opt}$ is clearly a non-monotonic function of P_{in}. Surprisingly, there are ranges of power inputs for which the homogenization times produced by the mixers $M_{2,3,4}^{opt}$ are equal to or higher than the homogenization times obtained by the same mixers at lower power inputs. These ranges are $1.2 \leqslant P_{in} \leqslant 2.3$ for mixer M_2^{opt}; $1.3 \leqslant P_{in} \leqslant 2.15$ for mixer M_3^{opt}; and $1.4 \leqslant P_{in} \leqslant 1.85$ for mixer M_4^{opt}, respectively. Clearly, these operating ranges of P_{in} should be avoided because a better or equal mixing performance can be achieved by using less power. The trend of the groups of curves in figure 6 suggests that mixers using a large enough number of modes should not present a range of high cost and low efficiency.

The non-monotonic behaviour of T_h versus P_{in} is due to the contribution of the stirring protocol optimization to the mixing performance of the mixers. This contribution can be clearly seen by comparing the curves corresponding to the switching time $\tau = 0.4$ in figures 4 and 6. First, the performance of all mixers substantially improves for low power inputs, i.e. in the range $1 < P_{in} \leqslant 1.3 \pm 0.1$. In this range, the protocol optimization prescribes the velocity fields $\boldsymbol{v}_0$ or $\boldsymbol{v}_1$ over one or two consecutive iterations, thus generating aperiodic protocols with optimal amounts of stretching and folding. The decrease in T_h is about 12 % for M_2^{opt} and about 25 % for $M_{3,4}^{opt}$. Second, little or no improvements are observed for power inputs higher than about 1.5 because, for this switching time and these power inputs, the protocol optimization tends to generate periodic protocols. In other words, for $P_{in} > 1.5$, the optimal mixers $M_{2,3,4}^{opt}$ perform as well as the mixers $M_{2,3,4}^{per}$.

Figure 6 shows that, in general, mixer M_4^{opt} performs better than M_3^{opt}, and the latter performs better than M_2^{opt}. The difference in performance is most visible in the range $1.0 \leqslant P_{in} \leqslant 3.0$, where the curves of T_h versus P_{in} corresponding to $M_{2,3,4}^{opt}$ are fairly well separated. The separation is largest at around $P_{in} = 1.7$, where the homogenization times generated by M_3^{opt} and M_4^{opt} are about 15 and 25 % less than the time induced by M_2^{opt}. In the upper range of power inputs, $3.0 < P_{in} \leqslant 4.0$,

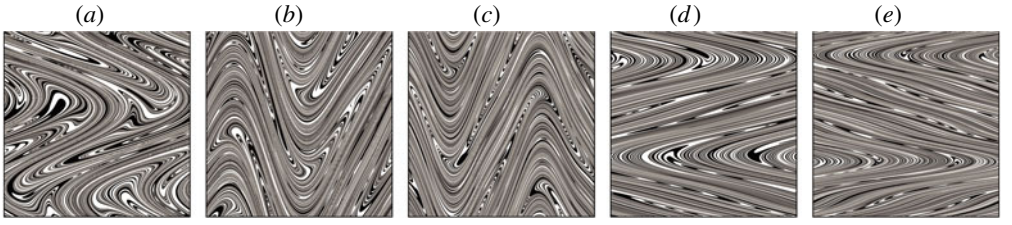

FIGURE 7. Snapshots at times (*a*,*b*) 4.4, (*c*) 4.0 and (*d*,*e*) 3.6 of the concentration field φ stirred by mixers (*a*) M_1^{opt}, (*b*) M_2^{opt}, (*c*) M_3^{opt} and (*d*,*e*) M_4^{opt} operating at switching time $\tau = 0.4$ and power inputs (*a*) $P_{in} = 1.0$, (*b–d*) 1.1 and (*e*) 1.3 when applied to the (*a–d*) 'envelope' and (*e*) 'vertical' initial configuration.

the curves tend to merge together and the performance of the mixer M_2^{opt} becomes competitive with the performance of the mixers $M_{3,4}^{opt}$. Apparently, for an achievable homogenization time, there is a trade-off between the number of modes used to resolve the stirring velocity profiles and the power input at which the mixers are operated. At low power inputs, shorter homogenization times are obtained by performing velocity profile optimization involving a larger number of modes, while at high power inputs the performance of the different mixers become similar and, consequently, the M_2^{opt} mixer is preferable. For example, $T_h = 3$ can be achieved by M_4^{opt} operating at $P_{in} = 2.5$ or by M_2^{opt} operating at $P_{in} = 3.8$.

One could suspect that some of the peculiar aspects of the performance of the mixers $M_{2,3,4}^{opt}$, depicted in figure 6, are an artifact of the measure chosen to quantify mixing, the mix-norm. This suspicion is unfounded. These peculiar aspects can be explained by analysing the lamellar structures of the mixture and the profile of the stirring velocity fields that generated them. Figure 6 shows that, as the power input increases from 1.0 to 1.1, the homogenization time decreases considerably with respect to the one generated by the mixer M_1^{opt}. The largest reduction, about 25 %, is obtained by M_4^{opt}, and the smallest, about 10 %, by M_2^{opt}. These substantial reductions are explained by the structure of the concentration fields shown in figure 7. When power input is equal to 1.0, the striations have a sinusoidal shape, which reflects the shape of the profile of the stirring velocity field, see figure 7(*a*), and the shear stress induced around the extrema of the profile is zero or very small. When the power input increases to 1.1, higher Fourier modes modify the fundamental mode, optimizing its shape and minimizing the regions where the shear stress is small. The wedge-shaped structures become sharper; see snapshots 7(*b–e*). Higher modes used in mixers $M_{3,4}^{opt}$ allow for a more precise control of the shape of the velocity profiles than M_2^{opt}; compare figure 7(*c*,*d*) to (*b*). Consequently, the optimized velocity fields generated by $M_{3,4}^{opt}$ induce more stretching, which produces up to 23 % reduction in the homogenization time at the cost of only 10 % increase in power consumption.

Even more intriguing is the fact that, when the power input is in the range $1.2 \leqslant P_{in} \leqslant 1.8$, an increase in the power input may result in the same or even lower mixing efficiency (see figure 6). This surprising result can be explained by examining the snapshots of the concentration fields and velocity profiles shown in figure 8. The snapshots in figure 8(*a–e*) are taken at time 3.2, and the corresponding velocity profiles in figure 8(*f–j*) were active during the eighth iteration of the Fourier sine flow, i.e. over the time interval $2.8 \leqslant t \leqslant 3.2$. As the power input increases, the amplitudes of the higher-order modes are forced to increase by the optimization constraints ((2.17) for M_2^{opt}, (2.19) and (2.20) for M_3^{opt}, and (2.22)–(2.25) for M_4^{opt}).

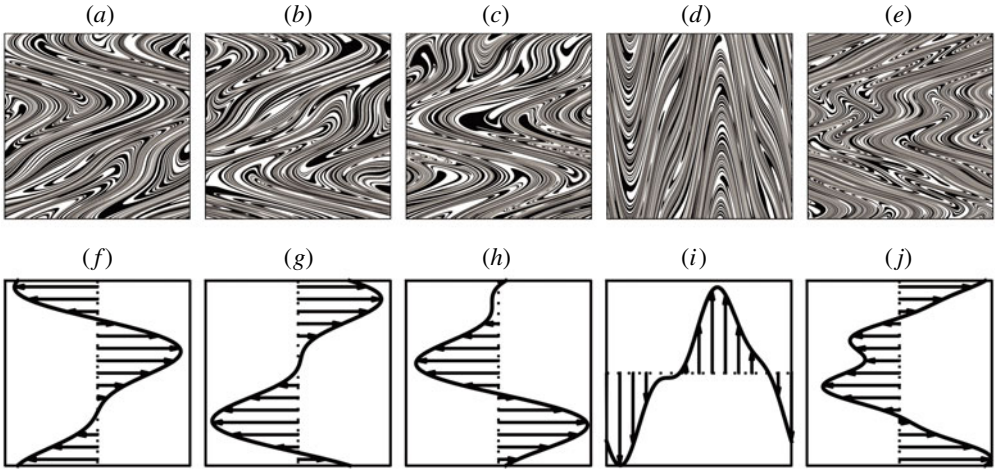

FIGURE 8. (*a–e*) Snapshots at time 3.2 of the concentration field φ stirred by mixers (*a–c*) M_2^{opt}, (*d*) M_3^{opt} and (*e*) M_4^{opt} operating at switching time $\tau = 0.4$ and power inputs (*a*) $P_{in} = 1.4$, (*b*,*d*,*e*) 1.5 and (*c*) 1.6 when applied to the 'vertical' initial configuration. (*f–j*) The corresponding shapes of the profiles of the stirring velocity fields used during the eighth iteration of the Fourier sine flow, i.e. during the time interval $2.8 \leqslant t \leqslant 3.2$.

The velocity profile optimization in general strives to generate profiles that induce high shear stress where it is most needed in the mixing domain. In this particular range of power inputs, however, the mixers are forced to create also regions of zero or very low shear stresses. Especially enlightening is the performance of the mixer M_2^{opt} operating at power inputs $P_{in} = 1.4$, 1.5 and 1.6. Figure 8(*f*,*h*) show that, owing to the optimization constraint (2.17), the creation of a region of high shear stress implies the creation of a region of almost zero shear stress, which, in turn, induces thick striations in the mixture; see figure 8(*a*,*c*). Clearly, the thickness of the lamellae increases as the power input increases from $P_{in} = 1.4$ to 1.6 and, consequently, induces an increase in the homogenization time T_h; see figure 6. Although shifted over the domain, the regions of almost zero shear stress are generated at each iteration of the Fourier sine flow. This can be clearly seen, for example, in figure 9, which shows the sequence of the velocity fields generated by the mixer M_2^{opt} applied to the 'vertical' initial configuration and operating at $\tau = 0.4$ and $P_{in} = 1.6$. In the case of mixers $M_{3,4}^{opt}$, the optimization procedure is able to use intelligently the third and fourth modes to minimize the regions of almost zero shear stress; see figure 8(*d*,*e*,*i*,*j*).

The mean computational costs of operating the mixers $M_{2,3,4}^{opt}$ are shown in figure 10. These mean costs are computed by averaging the costs involved in stirring the 'vertical' and the 'envelope' initial configurations. Note that the value of the computational cost $C = 26$ at $P_{in} = 1$ represents the cost of the mixer M_1^{opt}. The computational costs are nearly independent of P_{in} in the range $1.1 \leqslant P_{in} \leqslant 4$, and amount to about 300, 3000 and 30 000 evaluations of the cost function per iteration for M_2^{opt}, M_3^{opt} and M_4^{opt}, respectively. In other words, the computational cost results to be a fixed cost, which increases by an order of magnitude for each new mode added to the synthesis of the profile of the stirring velocity fields. Note that the mean computational cost of operating the optimal mixers $M_{2,3,4}^{opt}$ is about twice the cost of operating the periodic mixers $M_{2,3,4}^{per}$ because the coupled optimizations evaluate, at each iteration, the performance of both velocity fields, $\boldsymbol{v}_0$ and $\boldsymbol{v}_1$. This is a small cost to pay, considering

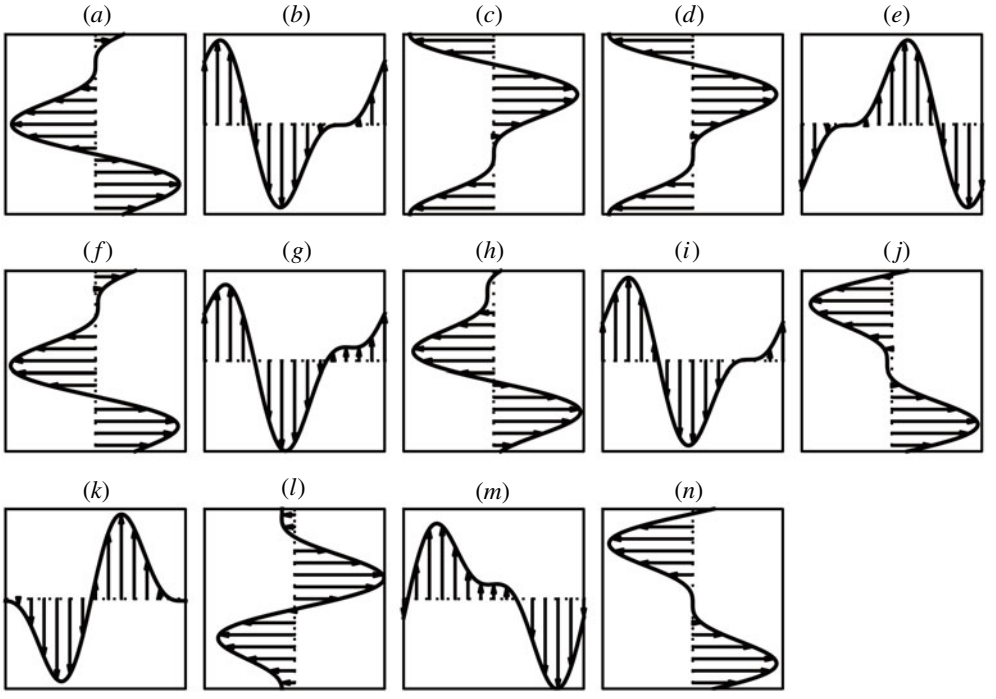

FIGURE 9. Profiles of the stirring velocity fields generated by the mixer M_2^{opt} applied to $\varphi_0 = V$ and operating at $\tau = 0.4$ and $P_{in} = 1.6$. Panels (a–n) correspond to the first 14 iterations of the Fourier sine flow.

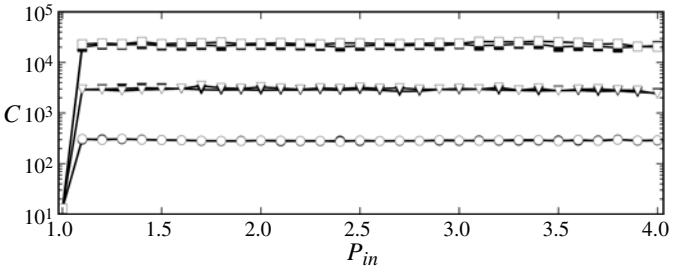

FIGURE 10. The computational cost of operating mixers M_2^{opt} (circles), M_3^{opt} (triangles) and M_4^{opt} (squares) operating at switching times $\tau = 0.2$ (filled symbols) and $\tau = 0.4$ (open symbols). The computational cost is the average of the costs involved in stirring the 'vertical' and 'envelope' initial configurations. The cost of operating M_1^{opt} is shown at $P_{in} = 1.0$.

that all mixers become optimal and present a much improved performance at low power inputs.

Figure 11 shows the total energy needed by the mixers $M_{2,3,4}^{opt}$ to obtain the target level of homogenization. Since the curves are segregated into three groups, according to the number of Fourier modes used, we can conclude that the total energy consumption is independent of the switching time and the geometry of the initial configuration. One can see that, under most operating conditions, the mixer M_4^{opt} needs less energy for obtaining the desired level of homogenization than the mixer M_3^{opt},

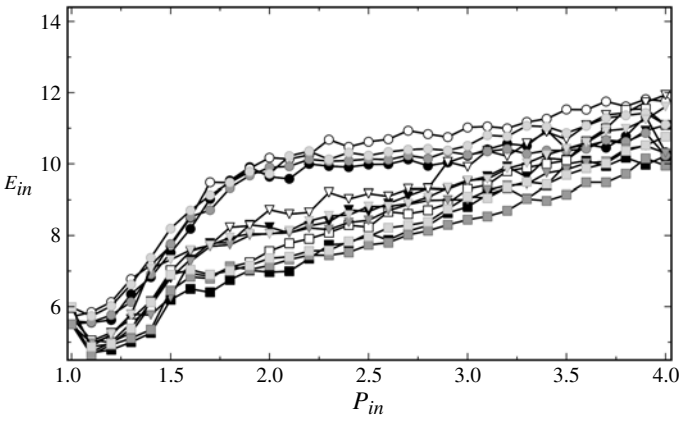

FIGURE 11. The energy needed for obtaining the target homogenization μ_h by mixers M_2^{opt} (circles), M_3^{opt} (triangles) and M_4^{opt} (squares) versus power input P_{in}. Black and white symbols correspond to $\tau = 0.2$ and indicate cases $\varphi_0 = V$ and $\varphi_0 = E$, respectively. Dark- and light-grey symbols correspond to $\tau = 0.4$ and indicate cases $\varphi_0 = V$ and $\varphi_0 = E$, respectively. The total energy consumption needed for operating the mixer M_1^{opt} is shown at $P_{in} = 1.0$.

which, in turn, needs less energy than M_2^{opt}. The most surprising aspect is that, at low power inputs, $1 < P_{in} < 1.3 \pm 0.1$, the total energy consumption of the mixers $M_{2,3,4}^{opt}$ is less than the energy required by the mixer M_1^{opt}. Consequently, for these power inputs, it is possible to obtain substantial reductions of the homogenization time, about 12 % for M_2^{opt} and about 25 % for $M_{3,4}^{opt}$, while requiring less energy than for M_1^{opt} (compare figures 6 and 11) if one is willing to pay the higher computational cost. As power input increases, the total energy consumption sharply increases in correspondence with the ranges of power inputs for which the homogenization times produced by the mixers $M_{2,3,4}^{opt}$ are equal to or higher than the homogenization times obtained by the same mixers at lower power inputs, i.e. $1.2 \leqslant P_{in} \leqslant 2.3$ for mixer M_2^{opt}, $1.3 \leqslant P_{in} \leqslant 2.15$ for mixer M_3^{opt} and $1.4 \leqslant P_{in} \leqslant 1.85$ for mixer M_4^{opt}, respectively. Clearly, these ranges of power input should be avoided because, within these ranges, the mixers $M_{2,3,4}^{opt}$ generate larger homogenization times while consuming a larger amount of energy than at lower power inputs.

At higher power inputs, i.e. $P_{in} > 1.75 \pm 0.2$, figure 11 shows that the total energy consumption grows at a constant rate, faster for the mixer M_4^{opt}, medium for the mixer M_3^{opt} and lower for the mixer M_2^{opt}. The curves come together for $P_{in} > 3.5$. In this range of power inputs, the mixer M_2^{opt} is the most cost-efficient of the three: it generates a homogenization time and requires a total energy about the same as mixers $M_{3,4}^{opt}$ for a computational cost that is two orders of magnitude lower. With respect to mixer M_1^{opt}, the mixer M_2^{opt} generates the target homogenization in half the time, while requiring twice the total energy. The computational cost is 10 times higher, which could become negligible in the near future considering that computer power is continuously increasing while its cost keeps decreasing.

4. Summary and conclusions

In this study, we estimated the cost efficiency of the mixing optimization of a new prototypical flow, the Fourier sine flow, which was obtained by extending the sine flow. The Fourier sine flow mixes a mixture on a two-dimensional torus by blinking,

at prescribed switching times, two orthogonal velocity fields whose profiles are represented by a Fourier series. We derived a family of mixers $M^{\alpha}_{1,2,3,4}$ of increasing complexity by truncating the Fourier series to one, two, three and four Fourier modes. Mixers using more than four modes are at the present time computationally too expensive.

We considered two types of optimization: the optimization of the velocity profiles and the optimization of the stirring protocol. We implemented the former by computing, at each iteration, the amplitudes and phase shifts of the Fourier modes that maximize the quality of mixing, measured using the mix-norm. We implemented the latter by selecting, at each iteration, the best performing of the two stirring velocity fields, i.e. the velocity field that minimizes the mix-norm.

To obtain a physically meaningful formulation of the optimization problem, we constrained the kinetic energy of the flow to be the same among all mixers and used the viscous dissipation as an estimate of the power input needed to operate the mixers. We discussed the performance of the mixers operating within the range of the feasible power inputs, $1 \leqslant P_{in} \leqslant 4$, common to the mixers $M^{\alpha}_{2,3,4}$. We characterized the performance of the mixers using three cost functions: the homogenization time, i.e. the time needed to achieve a target level of homogenization, the computational cost of the optimization and the total energy consumption, i.e. the energy required to operate the mixer to obtain a target level of homogenization. We neglected molecular diffusion in assessing the mixing performance of the mixers because the homogenization times targeted in this work are of the order of a few characteristic advection times, over which mixing by diffusion is negligible. We considered only two representative and challenging switching times, $\tau = 0.2$ and 0.4, for which the traditional sine flow cannot obtain the target homogenization even after thousands of iterations.

First, we characterized the performance of the mixers equipped with the velocity profile optimization and periodic stirring protocol. We found that all mixers $M^{per}_{1,2,3,4}$ perform considerably better at the moderate switching time, $\tau = 0.4$, than at the low switching time, $\tau = 0.2$. Apparently, the velocity profile optimization alone, independently of the number of Fourier modes used, is not able to guarantee a uniform performance of the mixers over the switching times chosen. In other words, the homogenization time depends on the switching time used to operate the mixer. Hence, mixers equipped with the velocity profile optimization alone are not optimal in the sense defined by Gubanov & Cortelezzi (2010) and, consequently, their cost efficiency cannot be fairly assessed. This deficiency is particularly evident at low switching times, i.e. $\tau \leqslant 0.2$, where the velocity profile optimization produces an unnecessary amount of folding in an attempt to compensate for the lack of stretching. At moderate and higher switching times, i.e. $\tau \geqslant 0.4$, the mixers perform much better and generate lower homogenization times because these switching times allow the periodic stirring protocol to produce a larger amount of stretching. Two positive aspects are observed: the performance of the mixers is nearly independent of the initial geometry of the concentration field, and their computational cost is independent of the power input used to operate them.

Next, we assessed the performance and cost efficiency of the mixers equipped with the velocity profile optimization coupled with the stirring protocol optimization. We showed that the mixers $M^{opt}_{1,2,3,4}$ perform equally well at low and moderate switching times, and their mixing performance depends only on the number of Fourier modes used. This is made possible because the velocity profile optimization delivers an optimal amount of shear where it is most needed in the domain while the stirring protocol optimization generates the optimal amount of stretching. The coupled action

of the two optimizations delivers an optimal amount of stretching and folding compatibly with the number of Fourier modes used and the selected switching time. The mixers $M^{opt}_{1,2,3,4}$ are hence optimal in the sense defined by Gubanov & Cortelezzi (2010) and, consequently, their cost efficiency can be fairly assessed. Surprisingly, the homogenization time generated by the mixers $M^{opt}_{2,3,4}$ is a non-monotonic function of the power input. For each mixer, there are ranges of power inputs for which the homogenization times are equal to or higher than the homogenization times obtained by the same mixers at lower power inputs. Clearly, these ranges of P_{in} have high cost and low efficiency and should be avoided. This result indicates that one cannot rely on the intuitive notion that higher power inputs produce faster homogenization times, not even when stirring protocol and velocity profiles are optimized. The total energy needed to operate the mixers $M^{opt}_{2,3,4}$ is a source of further surprises. In fact, at low power inputs, mixers $M^{opt}_{2,3,4}$ can be operated at lower energy than mixer M^{opt}_{1} while producing faster homogenization times than mixer M^{opt}_{1}.

The results presented for the Fourier sine flow allow us to draw some important conclusions about optimized egg-beater type of flows that could provide guidance for the development of optimal mixers in engineering applications.

(*a*) Mixers equipped with the velocity profile optimization and a periodic stirring protocol cannot be optimal, i.e. their performance depends on the switching time chosen independently of the number of Fourier modes used in the optimization. At low switching times, the egg-beater flows can generate an appropriate amount of stretching only by applying a stirring velocity field in the same direction over consecutive switching times, which is impossible when using periodic stirring protocols.

(*b*) The computational cost of the optimizations is independent of the power input at which the mixers are operated. The computational cost depends only on the number of Fourier modes used to optimize the profile of the stirring velocity fields. The computational cost grows by about an order of magnitude for each Fourier mode added to the optimization.

(*c*) For power inputs 10–30 % higher than the minimum power input, it is possible to produce an attractive reduction of the homogenization time in combination with a reduction of the total energy required to obtain it. The reduction of homogenization time and total energy increases as the number of Fourier modes used in the velocity profile optimization increases.

(*d*) Increasing the power input does not necessarily generate a reduction of the homogenization time. There are ranges of power inputs, from 40 to 80 % higher than the minimum power input, depending on the switching time, for which the mixers generate higher homogenization times and consume a larger amount of total energy than the same mixers do when operating at lower power inputs.

(*e*) In general, mixers using a higher number of Fourier modes generate faster homogenization times while requiring a lower amount of total energy and higher computational cost. However, for high enough power inputs, 300 % or more of the minimum power input, the optimal mixers perform similarly and, consequently, mixers implementing velocity profile optimization using only two Fourier modes are computationally more cost-efficient than mixers using a larger number of modes.

Acknowledgements

Funding was provided by NSERC under a Postgraduate Scholarship and under Contract No. RGPIN217169.

REFERENCES

ALVAREZ, M. M., MUZZIO, F. J., CERBELLI, S., ADROVER, A. & GIONA, M. 1998 Self-similar spatiotemporal structure of intermaterial boundaries in chaotic flows. *Phys. Rev. Lett.* **81**, 3395–3398.

ANTONSEN, T. M. JR., FAN, Z., OTT, E. & GARCIA-LOPEZ, E. 1996 The role of chaotic orbits in the determination of power spectra of passive scalars. *Phys. Fluids* **8**, 3094–3104.

BIGIO, D. I. & CONNER, J. H. 1995 Principal directions as a basis for the evaluation of mixing. *Polym. Engng Sci.* **35**, 1527–1534.

CORTELEZZI, L., ADROVER, A. & GIONA, M. 2008 Feasibility, efficiency and transportability of short horizon optimal mixing protocols. *J. Fluid Mech.* **597**, 199–231.

D'ALESSANDRO, D., DAHLEH, M. & MEZIĆ, I. 1999 Control of mixing in fluid flow: a maximum entropy approach. *IEEE Trans. Autom. Control* **44**, 1852–1863.

GUBANOV, O. & CORTELEZZI, L. 2009 Sensitivity of mixing optimization to the geometry of the initial scalar field. In *Analysis and Control of Mixing with an Application to Micro and Macro Flow Processes* (ed. L. Cortelezzi & I. Mezić). *CISM Courses and Lectures*, vol. 510. Springer.

GUBANOV, O. & CORTELEZZI, L. 2010 Toward the design of an optimal mixer. *J. Fluid Mech.* **651**, 27–53.

KHAKHAR, D. V., RISING, H. & OTTINO, J. M. 1986 Analysis of chaotic mixing in two model systems. *J. Fluid Mech.* **172**, 419–451.

KOLDA, T. G. 2005 Revisiting asynchronous parallel pattern search for nonlinear optimization. *SIAM J. Optim.* **16** (2), 563–586.

LAMBERTO, D. J., ALVAREZ, M. M. & MUZZIO, F. J. 2001 Computational analysis of regular and chaotic mixing in a stirred tank reactor. *Chem. Engng Sci.* **56**, 4887–4899.

LEWIS, R. M. & TORCZON, V. 2000 Pattern search methods for linearly constrained minimization. *SIAM J. Optim.* **10**, 917–941.

LIN, Z., THIFFEAULT, J.-L. & DOERING, C. R. 2011 Optimal stirring strategies for passive scalar mixing. *J. Fluid Mech.* **675**, 465–476.

LIU, M., MUZZIO, F. J. & PESKIN, R. L. 1994 Quantification of mixing in aperiodic chaotic flows. *Chaos, Solitons Fractals* **4**, 869–893.

MALVERN, L. E. 1969 *Introduction to the Mechanics of a Continuous Medium*. Prentice-Hall.

MATHEW, G., MEZIĆ, I., GRIVOPOULOS, S., VAIDYA, U. & PETZOLD, L. 2007*a* Optimal control of mixing in Stokes fluid flows. *J. Fluid Mech.* **580**, 261–281.

MATHEW, G., MEZIĆ, I. & PETZOLD, L. 2005 A multiscale measure for mixing and its applications. *Physica* D **211**, 23–46.

MATHEW, G., MEZIĆ, I., SERBAN, R. & PETZOLD, L. 2007b Optimization of mixing in an active micromixing device. In *Technical Proceedings of the 2004 NSTI Nanotechnology Conference and Trade Show*, Vol. 1. chapter 7. pp. 300–303. Nano Science and Technology Institute, Cambridge, MA. 6/8/2007.

MATHEW, G., PETZOLD, L. & SERBAN, R. 2002 Computational techniques for quantification and optimization of mixing in microfluidic devices. *Tech. Rep.* UCRL-JC-148966. Lawrence Livermore National Laboratory, July 2002.

MUZZIO, F. J., ALVAREZ, M. M., CERBELLI, S., GIONA, M. & ADROVER, A. 2000 The intermaterial area density generated by time- and spatially periodic 2D chaotic flows. *Chem. Engng Sci.* **55**, 1497–1508.

OTTINO, J. M. 1989 *The Kinematics of Mixing: Stretching, Chaos, and Transport*. Cambridge University Press.

PHELPS, J. H. & TUCKER, C. L. 2006 Lagrangian particle calculations of distributive mixing: limitations and applications. *Chem. Engng Sci.* **61**, 6826–6836.

PIERREHUMBERT, R. T. 1994 Tracer microstructure in the large-eddy dominated regime. *Chaos, Solitons Fractals* **4**, 1091–1110.

SZALAI, E. S., KUKURA, J., ARRATIA, P. E. & MUZZIO, F. J. 2003 Effect of hydrodynamics on reactive mixing in laminar flows. *Am. Inst. Chem. Engrs J.* **49**, 168–179.

THIFFEAULT, J.-L., DOERING, C. R. & GIBBON, J. D. 2004 A bound on mixing efficiency for the advection–diffusion equation. *J. Fluid Mech.* **521**, 105–114.

VIKHANSKY, A. 2002*a* Control of stretching rate in time-periodic chaotic flows. *Phys. Fluids* **14**, 2752–2756.

VIKHANSKY, A. 2002*b* Enhancement of laminar mixing by optimal control methods. *Chem. Engng Sci.* **57**, 2719–2725.